

Development and Calibration of Detonation-Driven High-Enthalpy and Hypersonic Test Facilities

Zonglin Jiang and Hongru Yu

1 Introduction

Hypersonics for the foreseeable future is the domain of space access and hypersonic flight. A hypersonic vehicle encounters an aero-thermodynamic environment characterized by strong shocks and high temperatures, and the flow in the hypersonic regime behaves quite differently from that at supersonic Mach numbers [1–3]. The kinetic energy associated with hypersonic flight is converted into internal energy which increases the temperature of the air and gives rise to endothermic reactions, such as vibration, dissociation and ionization of the air near the vehicle surface. Thus, the air becomes a gaseous reacting flow. The mechanisms behind this conversion include adiabatic compression and viscous energy dissipation. Heat is transferred from the surrounding high temperature air to the vehicle surface. The rate at which heat is transferred to the surface depends upon many factors, including the free-stream conditions, the configuration of the vehicle and its orientation to the flow, the temperature difference between the air and surface, and the surface catalysis. The aforementioned phenomena are different from those in supersonic flows and so called the real gas effects, which vary with the flight Mach number and altitude. Hypersonic reflects the close coupling of the aerodynamic forces with the heating environment and its research is the frontier of gas dynamics [4, 5]. Actually, it represents the fullest integration of both scientific fundamentals and engineering applications into “aerospace” systems full of challenges.

Hypersonic vehicles have been designed and built since the 1950s. In many of these programs, flight tests have revealed problems that had not been predicted either through analysis/computation or through ground-based testing. These problems exposed hypersonic flow phenomena not previously identified, what we shall

Z. Jiang (✉) · H. Yu

State Key Laboratory of High Temperature Gas Dynamics (LHD), Institute of Mechanics,
Chinese Academy of Sciences (CAS), 100190 Beijing, China
e-mail: zljiaang@imech.ac.cn

call “unknown unknowns” [4]. The severity of the hypersonic flight environment strongly depends on the mission profile and the vehicle configuration. Figure 1 shows typical trajectories of various spacecrafts and the regions of different physical and chemical processes in the shock layer near such vehicles [6]. It is important to note that the hypersonic flight regime covers a large range of speed and altitude. As an example, an air-breathing hypersonic vehicle must operate at relatively low altitudes in order to maintain the relatively high dynamic pressures required for maximum engine performance, therefore it often flies at Mach numbers 5–10 and altitudes from 30 to 50 km, as indicated in Fig. 1 where the aero-thermal-environment is dominated by fluid dynamics effects. Although the real gas effect is weak in these cases, the vehicle heating is high at leading edges, in the regions with shock interactions, and in downstream locations where the flow transitions to turbulence. Since there is considerable uncertainty in the boundary-layer transition prediction and since the convective heating from a turbulent boundary layer is much greater than that from a laminar boundary layer, this transition uncertainty presents critical challenges to the researchers. On the other hand, a high speed planetary entry blunt vehicle, such as the Galileo probe entering Jupiter or a high speed Earth return capsule, encounters an aero-thermal-environment dominated by high enthalpy effects. A high enthalpy flow in planetary entry is characterized by elevated levels of ionization and may result in significant radiation and heating. The strong real gas effects and low density effects also play an important role in the flight regime. As depicted in Fig. 1, the middle part of the typical trajectories of various spacecraft is for TSTO, and ascent and re-entry vehicles. Strong real gas effects dominate the flow around the vehicles.

In order to design new hypersonic vehicles, it is important to develop hypervelocity test facilities for ground-based experimental research. No single ground-test facility can fully simulate all aspects of hypersonic flight. The flow duration,

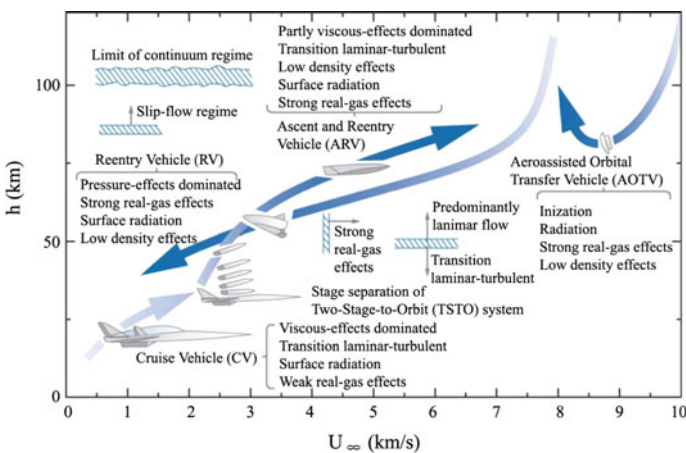


Fig. 1 Typical trajectories of various spacecraft and major aero-thermodynamic effects [6]

velocity, gas chemistry effects, Mach number, altitude or Reynolds number, model surface temperature, ablation effects, and the quality of the free-stream flow cannot be controlled simultaneously in any single facility, if at all. Nearly all tunnels suffer from noise levels much higher than in flight, and all tunnels simulating gas chemistry effects also have free-stream chemistry contaminants. Ground test simulations are an exercise in the art of combining partial simulations, each having unique advantages and disadvantages. After more than 60 years developments, high-enthalpy and hypervelocity test facilities suitable for studying aerothermochemistry are still based on shock tunnels [7]. Three main kinds of high enthalpy shock tunnels have been developed over the world for several decades. The first one is the heated-light-gas driven shock tunnel [8–10]. The second one is the free-piston driven high-enthalpy shock tunnel [11–15], and the third is the detonation-driven high-enthalpy shock tunnel [16–19]. During the last decades, many such hypervelocity test facilities have been built over the world and a lot of valuable experimental data have been produced, which are very precious for hypersonic study.

For hypersonic shock tunnels, one of the great challenges is to create a true hypersonic environment at a reasonable scale on the ground due to the high energy requirement. The detonation driver was first proposed to solve this problem by Bird in 1957 [16]. Later, a 13.3 m long detonation driver was built by Yu [17]. Grönig et al. developed TH2 in Aachen, Germany and the TH2 shock tunnel is operated in the backward-running detonation mode [18, 19]. Then in 1994, the bigger detonation-driven shock tunnel, so-called HYPULSE was setup in GASL, USA. It could be also operated as an expansion tube [7]. These detonation-driven shock tunnels can be operated either in the backward-running detonation mode to achieve stable test flows with long driving time at a relatively low enthalpy level or in the forward-running detonation mode to obtain high-enthalpy flows, but with a short test duration [20–22]. The recent rapid progress shows that the detonation-driven hypersonic test facilities become a promising method for hypersonic vehicle ground tests.

In the following sections, the research progress in the detonation-driven hypersonic test facilities developed in the State Key Laboratory of High Temperature Gas Dynamics (LHD), Institute of Mechanics, Chinese Academy of Sciences (CAS) is summarized, and the report includes the detonation-driven high-enthalpy shock tunnel (JF10), the long-test-duration hypervelocity detonation-driven shock tunnel (JF12) [24, 28] and the detonation-driven orbital-speed expansion tube (JF16). JF10 shock tunnel is operated for Mach numbers from M10 to 20, JF12 shock tunnel performance covers $M = 5\text{--}9$, and JF16 expansion tube is capable of producing the near orbital speed flow at $M = 20\text{--}25$. With these facilities, the typical trajectories of various spacecrafts could be covered so that research on aero-thermo-dynamics and hypersonic propulsion could be carried out in the laboratory to gain fundamental understanding on hypersonics.

2 Detonation-Driven High-Enthalpy Shock Tunnel JF10

The JF10 shock tunnel was developed by Yu in 1998 [17] for exploring re-entry physics and it could be operated both in forward- and backward-running detonation modes. In order to achieve high quality test flows at high enthalpy level, the JF10 shock tunnel was improved by replacing the forward-running detonation driver with a new FDC (Forward-running Detonation Cavity) driver [21] in 2003 and its performance tests were completed in 2006. Tunnel calibration results presented in this section include the improvement work on the JF10 shock tunnel, P5 pressure variations, the experimental data on nozzle flow uniformity and the incident shock decay in the driven section [23]. The experimental data have shown that the improvement on the JF10 shock tunnel is successful and future research work will benefit from the thus-obtained high quality hypersonic test flows.

2.1 Layout of the JF10 Shock Tunnels

The original and the improved JF10 shock tunnels are schematically shown in Fig. 2. The improved JF10 shock tunnel, as shown in Fig. 2b, consists of three main parts. The first part is the FDC driver being about 6.225 m in length and 150 mm in diameter, the second part is a driven section being 12.5 m in length and 100 mm in diameter, and the last part is a conical nozzle with a 500 mm diameter exit. For the original JF10 shock tunnel, as shown in Fig. 2a, its driver section is 10 m in length, and it is about 4 m longer than the FDC driver. Other parts are the same as the improved JF10 shock tunnel. The cavity of the FDC driver is 300 mm in diameter and 2 m in length. The detailed research work on the FDC driver was reported by Jiang et al. [20, 21]. For high-enthalpy shock tunnels, the shorter driver section is quite effective in reduction of experimental costs and nozzle throat ablation.

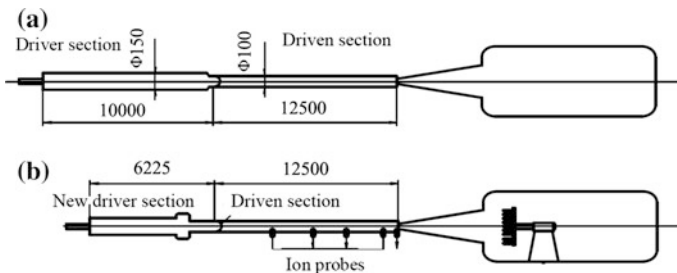


Fig. 2 Schematic of the improved and the original JF10 shock tunnels (length unit: millimeter)

2.2 Pressure Variations at the End of the Driven Section

For shock tunnels, P_5 pressure variation at the end of the driven section is a key parameter that indicates the test flow quality and stands for one of the most important performance parameter of shock tunnels. To obtain P_5 , the calibration experiments were carried out in the condition of $P_{4i} = 3.0$ MPa and $P_1 = 11$ kPa where P_{4i} and P_1 are initial pressures of the driver section and driven section, respectively. The incident shock Mach number is found to be 11.8 and the P_5 pressure history is plotted in Fig. 3.

Figure 3 shows the pressure history measured at the end of the driven section. This pressure profile acts as a measure of the reservoir pressure during nozzle working duration. The more stable the reservoir pressure is, the more uniform the nozzle flows becomes. From this figure, it is observable that the pressure level maintains approximately constant for more than 6 ms. By comparing it with the 2 ms test time achieved with the free piston driven shock tunnel, it is apparent that this pressure variation is very promising for extending effective test duration and demonstrated well the performance of the improved JF10 shock tunnel.

Figure 4 shows pitot pressure variations measured in the nozzle flow in the same experiment. The pressure profile looks similar to the reservoir pressure variation as shown in Fig. 3. The similarity agreement between these two pressure profiles indicates not only experimental data certification, but also effective test time possibly available from the improved JF10 shock tunnel. This time duration is not only long enough for both flow pressure and heat transfer measurements, but also provides good conditions for aerodynamic force tests with existing measurement instrumentations. As it is well known, stress force balances are very difficult for shock tunnel force measurements because of the short test duration. The results of aerodynamic force measurement will be more reliable if the shock tunnels could provide longer test duration. Therefore, a 6 ms long test duration is very useful for conducting aerodynamic force experiments.

Fig. 3 Pressure history measured at the end of the improved JF10 shock tunnel

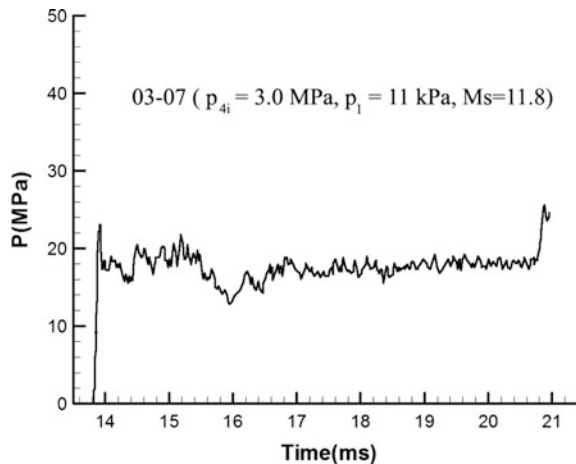


Fig. 4 Pitot pressure variations measured in the nozzle flow

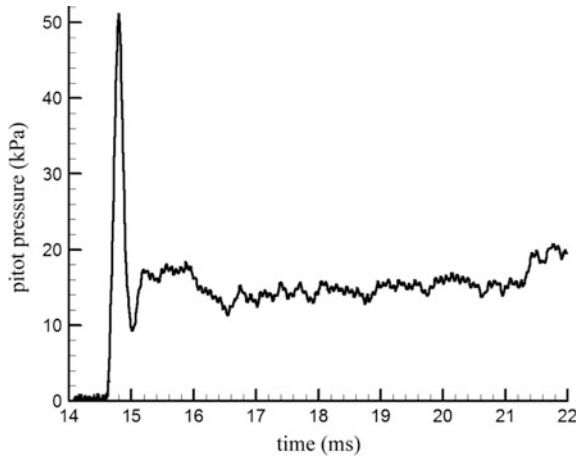
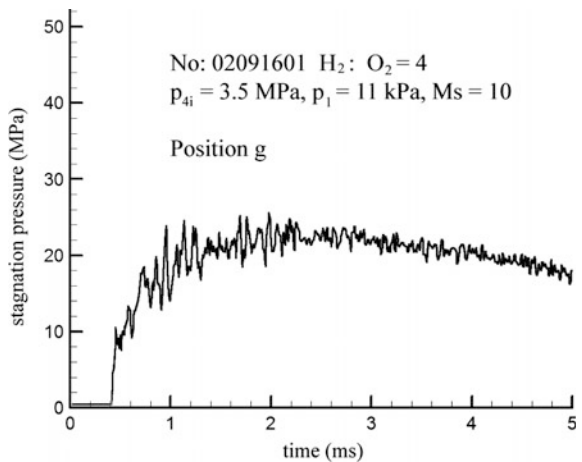


Fig. 5 Pressure variations measured at the end of the original JF10 shock tunnel



Similar performance tests were also conducted with the original JF10 shock tunnel and P_5 pressure variations measured at the end of the driven section are presented in Fig. 5. From the figure, it is observable that the test duration is about 3 ms before the pressure level decreases significantly. Considering that the 6 ms test duration was achieved in the improved JF10 shock tunnel with the shorter FDC driver, one can appreciate the progress achieved in detonation-driven high-enthalpy shock tunnel techniques by using the FDC driver.

2.3 Uniformity Test of Nozzle Flows

To examine out nozzle flow uniformity, five measurement positions in the JF10 nozzle flows are distributed along the nozzle centerline and the starting position is set at the nozzle exit. These positions are (a) $L = -50$ mm; (b) $L = 100$ mm;

(c) $L = 265$ mm; (d) $L = 400$ mm and (e) $L = 600$ mm, respectively. The experimental setup of pitot pressure measurements is shown in Fig. 6. Measurements were carried out at each measurement position both in the vertical and the horizontal directions. The measurement data were plotted together to demonstrate the flow uniformity of the nozzle.

Fig. 6 Experimental setup of pitot pressure measurements in the improved JF10 nozzle flow

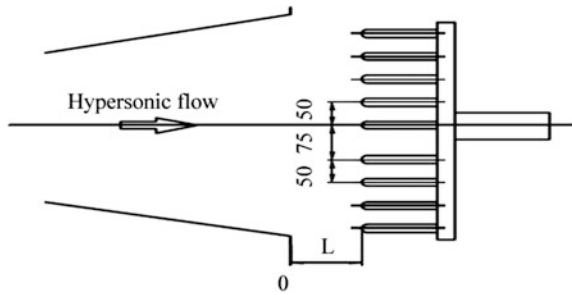


Fig. 7 Pitot pressure distributions in nozzle flows at two measurement positions in two directions

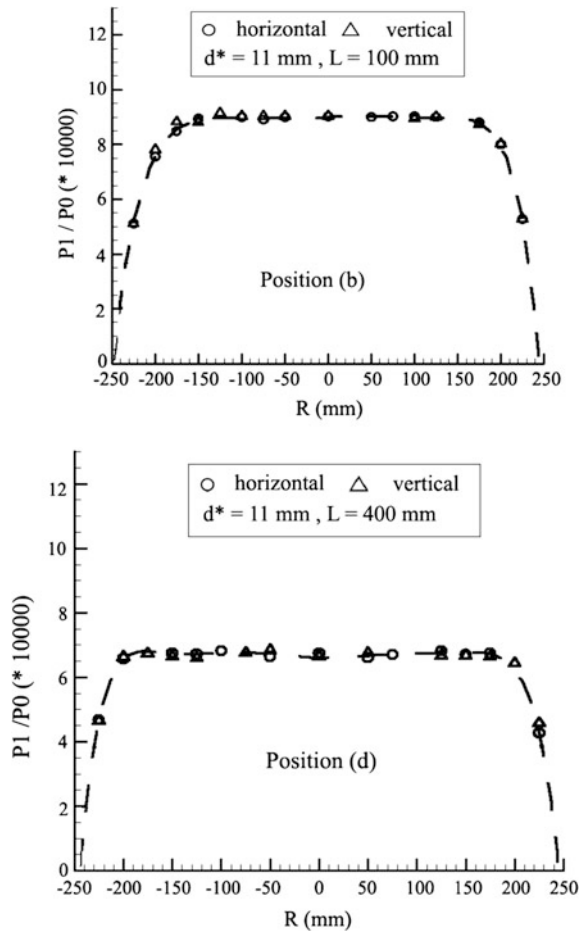


Figure 7 shows pitot pressure distributions in nozzle flows at two positions, i.e., (b) and (d). It is observable that the hypersonic flow in the nozzle central area appears quite uniform if evaluated from a view point of pitot pressure distribution. This uniform flow area is found to be approximately 700 mm in length and 400 mm in diameter. Although the pressure uniformity does not fully confirm hypersonic flow uniformity, these results are quite promising and very encouraging for showing nozzle flow quality.

2.4 Incident Shock Wave Decay

Incident shock decay in driven sections is an important parameter for demonstrating the performance of hypersonic test facilities since the test flow quality is affected considerably. For this investigation, three test cases were selected for comparison and the relevant test conditions are listed in Table 1. Cases A and B were carried out in the improved JF10 shock tunnel, and Case C was done in the original one, respectively. Experimental data from Case A and B are used to examine the incident shock decay at different initial conditions in detonation drivers, and Case C is used for the comparison between two different detonation drivers. The total flow enthalpy is kept to be almost the same in the three cases.

The incident shock speed is measured with several ion probes distributed along the driven section with equal intervals. The results of qualified tests for these ion probes are given in Fig. 8. The sign jumps occur sharply, which indicate the arrival of shock waves. Therefore, the incident shock speed could be calculated with high accuracy.

Figure 9 shows the incident shock decay rate along the driven section and the decay rate is determined by calculating Mach number drop per tube diameter, that is, the diameter of the driven section. By examining cases A and C, it can be seen that stronger incident shock waves can be driven out with the FDC driver and the Mach number could be 10 % higher in similar operating conditions. The incident shock decay in the improved JF10 shock tunnel is about 30 % less, and actually the decay rate is 3.04 % in case A and 3.94 % in case C. The experimental data of cases A and B are almost the same and this indicates that the initial pressure ratio of the driver and driven section has no significant effects on the incident shock decay if the total flow enthalpy is the same. Shock wave decay is weaker in Case A than that in Case C. This indicates that the FDC driver gives good performance.

Table 1 Test conditions for investigating the incident shock decay in the driven section

Test conditions	P_{4i} (MPa)	P_1 (KPa)	P_{50} (MPa)	T_{50} (K)
A	1.5	4.5	8.0	7480
B	3.0	11	19.4	7920
C	1.5	4.7	8.3	7200

Note P_{50} and T_{50} are the reservoir pressure and temperature, respectively

Fig. 8 Ion probe signs for incident shock speed measurement

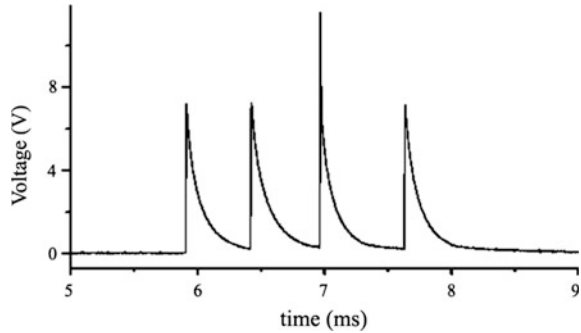
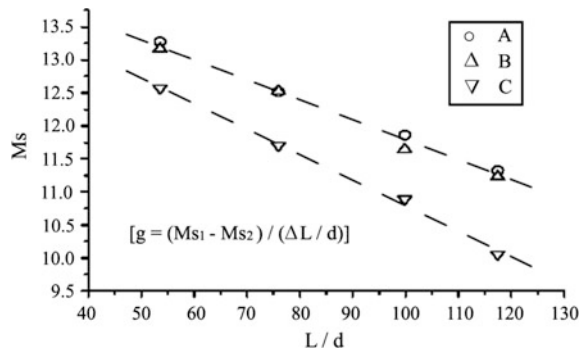


Fig. 9 Incident shock wave decay for three test cases



2.5 Concluding Remarks

From experimental data and the above discussions, the research progress on the detonation-driven high-enthalpy shock tunnel can be summarized as follows:

- (1) The improvement on JF10 shock tunnel with a new FDC driver was demonstrated to be very successful and a stronger incident shock could be generated with a lower decay rate in the similar initial conditions by comparing with the original JF10 shock tunnel.
- (2) The test duration of the improved JF10 shock tunnel was extended by two times even though the new FDC driver is 40 % shorter than the original forward-running detonation driver. The 6 ms test duration is achieved, which makes aerodynamic force measurements much easier.
- (3) The uniform core flow region of the improved tunnel is about 700 mm in length and 400 mm in diameter.

3 Detonation-Driven Hypervelocity Shock Tunnel JF12

Air-breathing hypersonic vehicles usually operate at relatively low altitudes in order to maintain the relatively high dynamic pressures required for maximum engine performance, and the scaling law is not valid due to the chemical reaction in its engine. Advanced hypersonic test facilities have been under development for more than 60 years [7], but there is still a lack of facilities for generating high-enthalpy flows with Mach numbers higher than $M = 7$ for hypersonic propulsion tests due to huge technological barriers in wind tunnel techniques, especially for the facility damage due to severe heat transfer problems for long test duration.

In order to meet the requirement of ground experiments of air-breathing hypersonic vehicles, several types of facilities were developed, including combustion-heated wind tunnels, arc-heated hypersonic wind tunnels, conventional air-heated wind tunnels and high-enthalpy shock tunnels. To clarify the real gas effect on hypersonic flows and the test-gas contamination effects on supersonic combustion, the shock tunnel appears to be the most promising test facility to provide hypersonic propulsion tests with the pure airflow of hypervelocity and the required total temperature. However, the test duration provided with shock tunnels is usually quite short and it is usually only a few milliseconds for most of the high-enthalpy shock tunnels. The short test-duration imposes severe technical barriers on the tests of supersonic combustion and aerodynamic force measurement. Moreover, it becomes even more difficult for hydrocarbon fuel combustion since the fuel injection, evaporation, mixing and ignition take time. Therefore, the development of the long test-duration shock tunnel is of significant importance for the study of air-breathing hypersonic vehicles.

A research project was launched in the State Key Laboratory of High Temperature Gas Dynamics (LHD), Institute of Mechanics, CAS in 2002 to investigate the techniques for long test-duration and hypervelocity shock tunnels. Much progress has been achieved successively since then. Jiang et al. [21] proposed a forward detonation cavity (FDC) driver, and the test duration has been prolonged to three times than the original one. Li et al. [26] investigated the wave/interface interaction in shock tubes, and the tailored condition was proposed for detonation-driven shock tunnels. The shock/boundary interaction near the end of the driven section was examined numerically in detail, and a steel ring is proposed to be installed around the nozzle throat by Li et al. in order to delay driver-gas mixing with test gases [27]. Wave-reflection damping in the vacuum tank is solved with an E-shaped configuration of the vacuum system. With these techniques and the backward-running detonation driver, a large hypervelocity detonation-driven shock tunnel has been designed and calibrated successfully. This shock tunnel, as shown in Fig. 10, is about 265 m in total length, and the diameter of the nozzle exit is 2.5 m [27].



Fig. 10 Photo of long-test-duration hypervelocity detonation-driven shock tunnel

3.1 Descriptions of the JF12 Shock Tunnel

Under the support of National Major Project of Scientific Instrumentation R&D, the Long-test-duration Hypervelocity Detonation-driven Shock Tunnel (LHDST) was developed based on the backward-running detonation driver with several innovative techniques by the end of May 2012, as shown by the photo in Fig. 10. The shock tunnel, JF12, is named after shock tunnels under the serial number in LHD laboratory. Professor Sasoh, from Nagoya University, suggested an endearment name of the hypervelocity detonation-driven real gas shock tunnel (Hyper-Dragon for short) to this facility after his visit. Its performance tests demonstrated that the facility is capable of reproducing the pure airflow with Mach numbers from 5 to 9 at altitude of 25–50 km with 100 ms test duration, and will be a useful tool for testing engine/frame-integrated hypersonic vehicles and investigating into fundamental physical issues in hypersonic and high-temperature gas dynamics.

Figure 11 shows schematically the entire system of the JF12 shock tunnel. From its right to left, the first part is the vacuum system for damping wave-reflection during nozzle starting process, and its vacuum tank with a volume of 600 m³ is 50 m in length. The second part is the test section that is 15 m in length and 3.5 m in diameter. The contoured nozzle is 15 m in length and 2.5 m in diameter, and another nozzle is smaller, having an exit of 1.5 m in diameter for Mach number of 5–7. Next to the nozzle, there is the driven section being 89 m in length and 720 mm in diameter. The detonation driver is 99 m in length and 400 mm in diameter. The driver operates in the backward-running detonation mode, that is, the

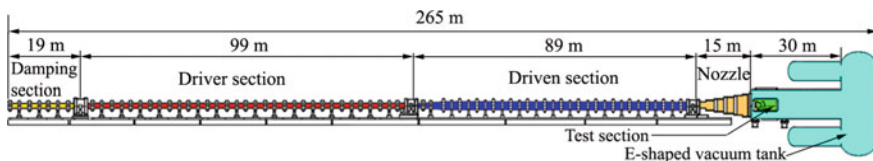


Fig. 11 Schematic of the long-test-duration hypervelocity detonation-driven shock tunnel

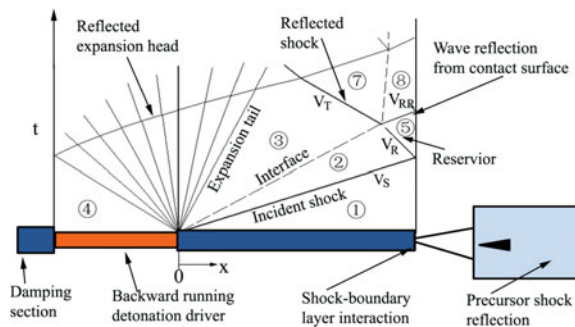
detonation is ignited at its right end. The detonation driver and the driven section are connected with the transient part by which the tube diameter is gradually reduced from 720 to 400 mm. Between the detonation driver and the transient part, there is the diaphragm rig that is used to produce the incident shock wave in the shock tunnel after the direct detonation initiation. The damping section is located at the far left end of the facility, and is 19 m in length and 400 mm in diameter.

For experimental measurements, the JF12 shock tunnel is equipped with a 384-channel digital data acquisition system that is able to acquire, amplify, digitize and store the data in real time. Immediately after each test run, the data are transferred to the computer in the control room for processing. Three 6-component force and moment balances are designed based on the 100 ms test duration and calibration experimental data showed that the balances work pretty well.

3.2 New Techniques Developed for the JF12 Shock Tunnel

A typical wave diagram for the detonation-driven shock tunnel operated in the backward-running detonation mode is shown in Fig. 12. The detonation is initiated between the detonation driver and the driven section, and its wave graph is schematically presented in Fig. 12. The nozzle starts once the incident shock is reflected from the reservoir end and the reservoir state is interfered when the reflected wave from the left end of the shock tunnel arrives. When building up a long test-duration and hypervelocity shock tunnel for Mach numbers of 5–9, there are several physical issues that affect the test time in different ways. These physical issues are briefly described as follows. The first issue is the powerful detonation driver, and the shock tunnel performance will benefit from the detonation driver with high pressure and required temperature. The second issue is the tailored interface operation condition and the wave reflection from the interface separating the driver gas from the test gas will ruin the test flow quality in an untailored operation condition. The third issue is the precursor wave reflection in the vacuum tank during the nozzle-working process, and the test duration will be terminated once reflected waves propagate into the test flow region. A large amount of laboratory space may

Fig. 12 Physical issues for developing long test-duration shock tunnel



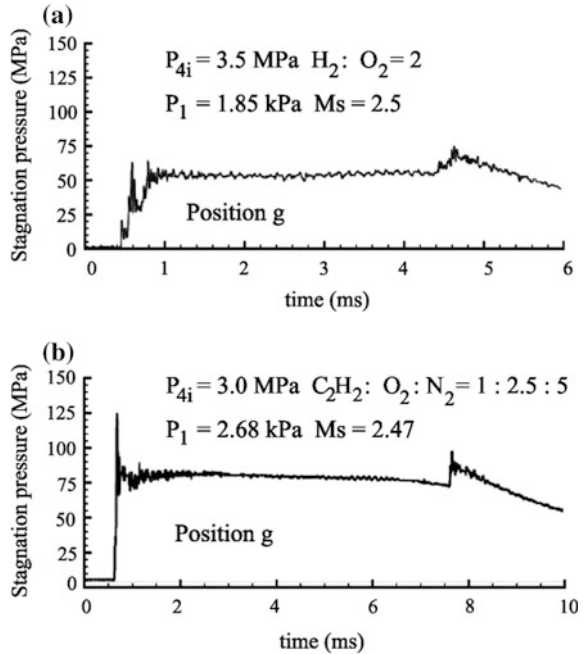
be occupied since the vacuum tank must be long enough to accommodate the wave propagation. Shock/boundary interaction is another key issue for shock tunnel test time. Immediately after the incident shock reflection, the driver gas moves within the boundary layer near the end of the driven section; leading to driver/driven gas mixing and result in test gas contamination. The last issue arises from the dumping section. The extremely high pressure from detonation front reflections must be carefully concerned in this section. These physical issues will be discussed in the following sections, and the corresponding techniques for constructing shock tunnels having long test-duration will also be discussed.

3.2.1 Backward-Running Detonation Driver

The backward-running detonation driver is well known to be good at producing a column of driver gas with uniform pressure regardless of the fact that its capability for incident shock generation is less powerful than the forward-running detonation driver. However, it is fully capable of producing hypersonic flows with Mach number from 5 to 10 because the required incident shock is not very strong. Furthermore, the total temperature of the test gas is about 1500–2300 K for the flows within a Mach number range of 5–7, and detonation drivers are usually too powerful to apply directly. Because the initial temperature of the test gas in front of the incident shock is the room temperature, the low temperature driver gas after detonations is required for the tailored interface operation that matches the sound speed of the driver gas with the test gas. Thus interface matching is extremely important to eliminate wave reflections from the contact face located between the driver gas and the test gas. On the other hand, the detonated driver gas must have high enough pressure to produce a strong incident shock, but not too high temperature for properly tailoring the interface condition. This is the key issue for developing a shock tunnel with long test time.

According to detonation physics, different detonable gas mixtures have different detonation temperature and pressure. The high detonation pressure driver gas with low temperature can be achieved by careful choice of the gas mixtures. Numerous gas mixtures were tested to examine the performance of a backward-running detonation driver by using the JF10 detonation-driven shock tunnel. Two results from the experimental data obtained are shown in Fig. 13, showing pressure variations during tunnel operation duration. Figure 13a shows P_5 of the hydrogen/oxygen gas mixture at the initial pressure of 3.5 MPa for the first case, and thus the generated incident shock has the Mach number of 2.5. Figure 13b presents the data of the acetylene/oxygen gas mixture at the initial pressure of 3.0 MPa for the second case, and the obtained incident shock Mach number is 2.47. It is observable that the pressure history shown in Fig. 13b reaches about 800 bars even though the P_1 is lower than the one in the second test case, and the P_5 value is 50 % higher than the one in Fig. 13a. Therefore, the backward-running detonation driver with the acetylene/oxygen gas mixture is suitable for generating hypersonic flows at the low Mach number region, that is, Mach number of 5–7, where the total temperature is not very high.

Fig. 13 Pressure variations obtained with a backward-running detonation driver at the same position for two test cases: **a** hydrogen/oxygen gas mixture; **b** acetylene/oxygen gas mixture



3.2.2 Tailored Interface Operation Condition

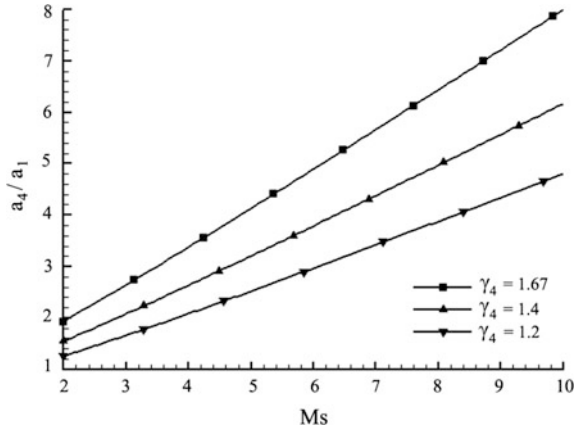
The second issue is the wave reflection from the contact surface that separates the driver gas from the driven gas. If the reflection takes place, the total pressure and temperature of the test gas at the end of the driven section will be changed during the nozzle operating, resulting in the early termination of shock tunnel test. In order to avoid the wave reflection, the sound speed of the test gas in front of the incident shock must meet a certain requirement for the sound speed of the detonation gas behind the contact interface. For the backward-running detonation drivers, the tailored interface condition is derived as follows:

$$\frac{a_4}{a_1} = \frac{2}{\gamma_1 + 1} \left(M_s - \frac{1}{M_s} \right) \left\{ \left[\frac{(\gamma_1 - 1)M_s^2 + 2}{2\gamma_1(M_s^2 - 1)} \right] \left[\gamma_4^2 + \frac{\gamma_1\gamma_4(\gamma_4 + 1)(M_s^2 - 1)}{(\gamma_1 + 1)M_s^2 + 2} \right]^{1/2} + \frac{\gamma_4 - 1}{2} \right\}$$

where a_4 is the sound speed of the detonated driver gas, γ_4 is its specific heat ratio, M_s is the incident shock Mach number, a_1 is the sound speed of the test gas behind the incident shock, and γ_1 is its specific heat ratio.

Based on the tailored-interface operation condition, calculated results are presented in Fig. 14, showing the relation between the sound speed ratio a_4/a_1 and the

Fig. 14 Sound speed ratio a_4/a_1 varying with the incident shock March number M_S under the tailored-interface condition for a backward-running detonation driver with different detonable gas mixtures

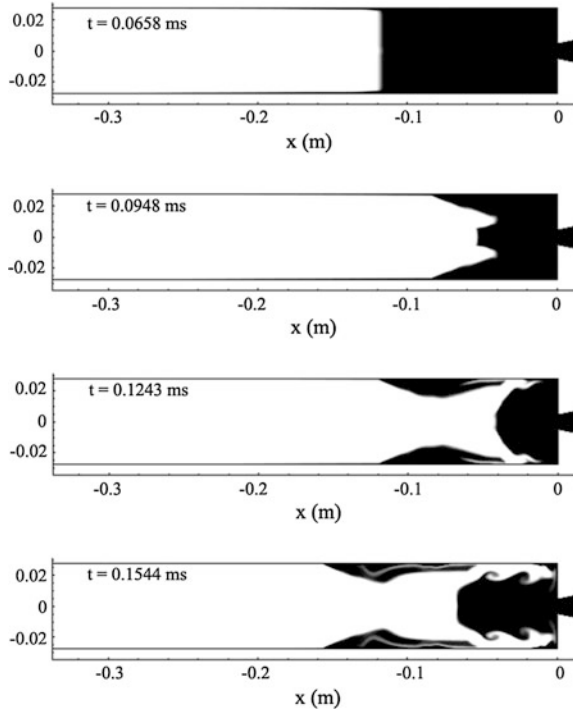


incident March number M_S . For most of the experiments, air is used as a test gas at ambient temperature, and the sound speed ratio can be adjusted only by selecting different detonable gas mixtures. For the given incident shock, the larger the specific heat ratio is, the higher is the sound speed ratio. The acetylene/oxygen gas mixture is suitable for the low Mach number of hypersonic flows, and the hydrogen/oxygen gas mixture is for the high Mach number. There is another way to adjust the sound speed ratio by applying a diverging section between the detonation driver and the driven section, as mentioned by Laderman [29], and with the diverging section the detonation driver can be extended to the low Mach number region of hypersonic flows since the driver operation is limited by the direct detonation ignition.

3.2.3 Gas Contamination from the Shock/Boundary Interaction

The third issue is the shock/boundary interaction near the end of the driven section. The boundary layer will develop while the incident shock propagates in the driven section, and the shock/boundary interaction will take place after the incident shock reflects. The phenomenon can cause contamination of the test gas and greatly affect the test-duration of shock tunnels. Numerical simulations are carried out for examining the problem and the obtained results are presented in Fig. 15. Figure 15 shows a time sequence of gas fraction distributions in which the white region stands for the driver gas while black stands for the test gas. From the figure, it is observable that the driver gas goes along the driven section wall, enters the nozzle throat much earlier than what is expected, and leaves a relatively large percentage of the test gas behind. The test gas contamination is a severe problem for shock tunnels and the test duration could be reduced significantly. To prevent fast entering of the driver gas into the nozzle throat, a steel ring is suggested to be mounted around the nozzle throat. Numerical simulations demonstrated that the test duration is increased by 50 % due to the steel ring installation.

Fig. 15 A time sequence of gas fraction distributions from mixing process of the driver and driven gases (*white* the driver gas and *black* the test gas)



3.2.4 Wave-Reflection Damping in the Vacuum Tank

The last issue to be discussed here is the reflection-wave damping in the vacuum tank. For shock tunnels, its test duration is usually proportional to its length. This is the reason why the test time for shock tunnels is short, only a few milliseconds. If one wants to develop a shock tunnel having a hundred millisecond test duration, the total length of the shock tunnel will be extremely long because the wave speed is very high. Reduction of the shock tunnel length and the associated laboratory space is a meaningful work to do. A number of different configurations of the vacuum system were numerically simulated, and the results from two configurations are presented in Fig. 16. The upper half of the figure shows the pressure distribution in the E-shaped vacuum tank and the lower half depicts the T-shaped one. The overall volume and the length for the two test cases are set to be approximately same in the calculations. It is demonstrated that the E-shaped vacuum system has the better performance than the T-shaped configuration. Therefore, the JF12 shock tunnel is equipped with an E-shaped vacuum tank with about 600 m^3 in volume. The performance test shows that more than 200 ms test-duration was achieved for $M = 7$ test flow with the E-shaped vacuum tank being 50 m in length.

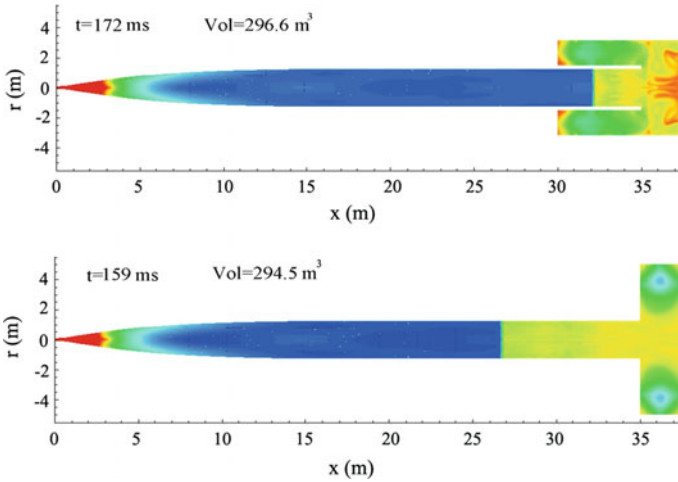


Fig. 16 Wave propagation and reflection in the E-shaped and T-shaped vacuum vacuums

3.3 The Results of Performance Tests

Using the above mentioned techniques, the project for the long-test-duration hypervelocity detonation-driven shock tunnel was initiated at the beginning of 2008, its installation was completed in March 2011, and the performance tests have been carried out since then. Some experimental data are presented in this chapter to show promising features of the JF12 shock tunnel.

Figure 17 presents reservoir pressure variations at the end of the driven section for a nozzle Mach number 7, and actually it is the P_5 pressure for the shock tunnel. The incident Mach number is measured to be 4.57. The total temperature of the test gas is about 2468 K, and the uniform pressure maintains as long as 130 ms. Figure 18 shows the pitot pressure variation at the nozzle exit in the test section for the same shot. The pitot pressure profile looks similar to the P_5 curve, and the test duration is confirmed.

The survey rake is made for the pitot pressure measurement, and is 2 m long in both vertical and horizontal directions. Forty pressure sensors are distributed along the rake in an equal interval. The sensors along the horizontal branch are numbered

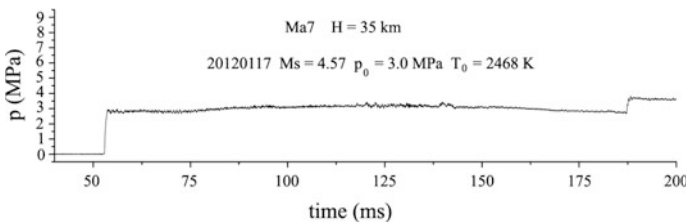


Fig. 17 Reservoir pressure (P_5) variation at the end of the driven section for nozzle Mach number 7

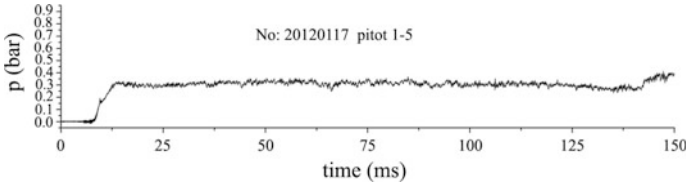


Fig. 18 Pitot pressure variation at the nozzle exit in the test section for nozzle Mach number 7

from left to right. The pressure profile in Fig. 18 is recorded by sensor No. 5. Experimental data from the pitot pressure survey are presented in Fig. 19. It is apparent from the figure that the pitot pressure near the boundary of the test flow is a bit higher than the one recorded in the central area. From the figure, it is concluded that the test flow region at the nozzle exit plane is about 2 m in diameter.

If the flight condition, for instance, for Mach number 8 at an altitude of 40 km is required to duplicate, 7 kg hydrogen gas must be filled into the driver section of the JF12 shock tunnel to reach the initial pressure of 2.5 MPa for the hydrogen-oxygen gas mixture. The hydrogen consumed for such a shot is about 18 bottles of compressed gas. If the light-gas driver is accepted for the JF12 shock tunnel, one shot will need about 380 bottles of hydrogen for the driver gas to reach an initial pressure of 14.2 MPa. The consumed driver gases estimated for the two drivers are given in Table 2. The heated-light gas driver is an important technique for shock tunnels, however, it may cause some problems for larger scale shock tunnels, not only the operation expenses become high, but heating, storage and transportation for a huge volume of light gases are very tough problems to deal with.

Fig. 19 Pitot pressure profile at the nozzle exit plane for Mach number 7

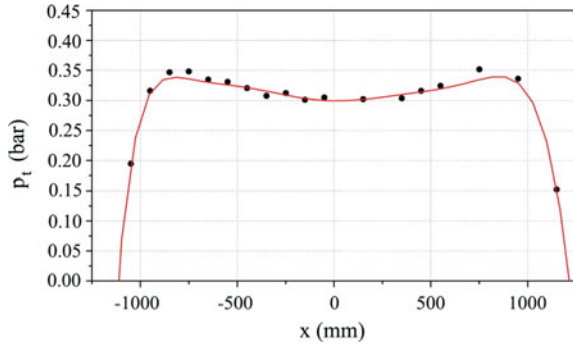


Table 2 Driver gas estimated for the detonation and light-gas drivers (for condition: H = 40 km and $M_\infty = 8$)

	Initial pressure (MPa)	Hydrogen	
		Weight (kg)	Bottles
Detonation driver	2.5	7	18
Light gas driver	14.2	152	380

Hydrogen bottle: $V = 0.04 \text{ m}^3$; $p = 12 \text{ MPa}$; $m = 0.4 \text{ kg}$

3.4 *Concluding Remarks*

The successful development of the long-test-duration hypervelocity detonation-driven shock tunnel was demonstrated with calibration tests. The shock tunnel performance was achieved due to the above discussed techniques, such as the detonation driver with the acetylene/oxygen mixture, the tailored-interface operation condition for detonation drivers, the shock/boundary interaction control at the end of the driven section, and the E-shaped configuration of the vacuum tank. The shock tunnel is capable of duplicating the flight conditions for Mach number 5–9 at the altitude of 25–50 km. Large scale test flows with more than 100 ms test duration can be generated at a reasonable operation expense. Hypersonic boundary layer development, scaled-model effects, hypersonic propulsion, vehicle-engine integrated models are possible to be tested with the new facility. It will be a useful tool for investigating into fundamental physics in hypersonic propulsion.

4 **Detonation-Driven High-Enthalpy Expansion Tube JF16**

Among the developed hypersonic test facilities, the high-enthalpy expansion tube appears to be a promising facility for generating near orbital speed flows for earth re-entry study. In the expansion tube, the unsteady flow expansion mechanism is applied to further speed up test gases to achieve high flow velocity, lower static temperature and less gas dissociation as compared with reflected shock tunnels. The concept of an expansion tube was proposed first by Resler and Bloxsom in 1952 [30]. Theoretical research was carried out later by Trimpi [31], but his experimental results showed that steady test flows were not achieved as was predicted. The Center for Hypersonics at the University of Queensland applied the free-piston driver to the expansion tube, and three expansion tubes, referred to as X1, X2, X3, were set up and a series of orbital speed experiments were carried out [32]. The JX-1 expansion tube with free-piston driver was built later by Sasoh at Tohoku University, Japan [33]. Based on the above introduced FDC driver [21, 23], the detonation-driven orbital-speed expansion tube, referred to as the JF16 expansion tube, was set up in 2006. The experimental data show that the velocity of the test gas reaches 8300 m/s. The test duration is around 50–100 μ s and the total flow enthalpy is about 40 MJ/kg [25].

4.1 *Descriptions of JF16 Expansion Tube*

The JF16 expansion tube is shown schematically in Fig. 20. It consists of five main parts: a FDC driver, a shock tube, an expansion acceleration section, a test section

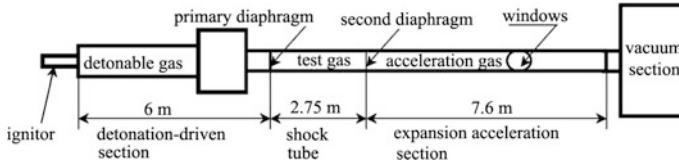


Fig. 20 Schematic of the JF16 expansion tube

and a vacuum section. This FDC driver is 6 m in length and 150 mm in inner diameter with an igniter installed at its left end to initiate a forward-running detonation. The driven shock tube is 2.75 m in length and 68 mm in inner diameter, and it can be replaced with a longer one of 4.75 m for different experimental requirements. The primary diaphragm is located between the FDC driver and the shock tube, separating the detonable gas mixture from the test gas. The expansion acceleration section is 7.6 m long with a square cross section of 60 mm \times 60 mm. The second diaphragm is placed between the shock tube and the expansion acceleration section, separating the test gas from the acceleration gas. A set of test windows opposing each other is installed in the expansion acceleration section for flow visualization. A vacuum section is added to the right end of the facility to weaken wave reflections for minimizing their effects on the generated hypervelocity flows.

Surface pressure measurements were carried out along the shock tube and the expansion acceleration section. By setting the position of the second diaphragm as a starting point, the distances to each pressure transducer are set to be 1612, 2447, 3247 and 3847 mm, which are named as B, C, D, and E, respectively in the order from left to right. Ten surface ion probes were distributed along the shock tube and the expansion acceleration section with an equal interval to obtain the incident shock speed. The detonable gas applied is a hydrogen/oxygen mixture at 4:1 ratio. The igniter is a small diameter tube to provide a certain amount of hot gas to the FDC driver to ensure a direct initiation, and the gas mixture in the igniter is initiated with explosion wires.

4.2 Test Flow Evaluation

In the performance tests, the shock tube and the expansion acceleration section were filled with air at 20 and 0.15 mm Hg, respectively, as a basic test case. For special cases, the condition changes will be explained explicitly if there is any difference in the initial conditions. The FDC driver was filled with the H_2/O_2 mixture at an initial pressure of 1.0 and 1.5 MPa, respectively for the first two test cases. The wall pressure variations related to the test flow quality are presented in Figs. 21 and 22 for discussion.

Figure 21 shows the pressure histories measured at four measurement points of the first test case where the initial pressure in the FDC driver is set to be 1.0 MPa.

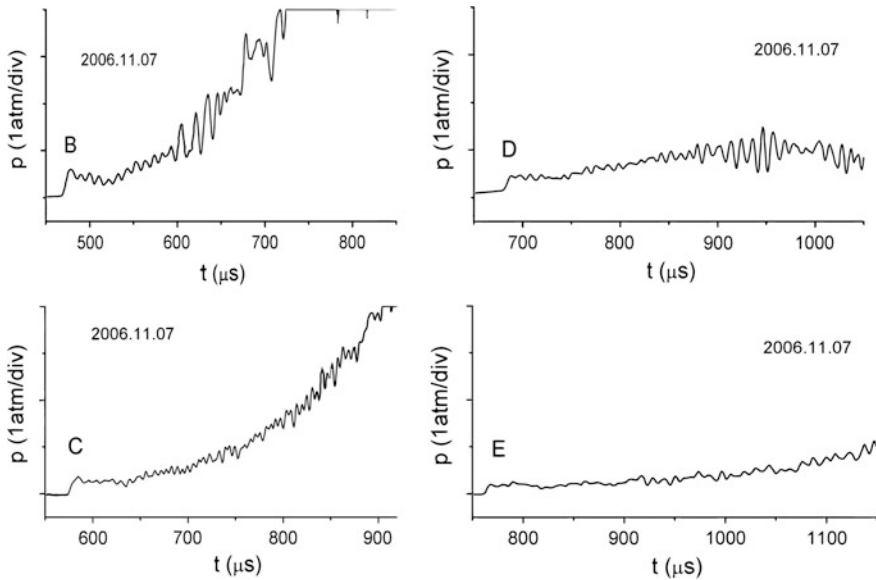


Fig. 21 Wall pressure histories at four measurement points under the initial conditions of 1.0 MPa in FDC driver, 20 mm Hg in the shock tube and 0.15 mm Hg in the acceleration section

It is observable that the pressure plateau appears behind the sharp jump induced by the incident shock at each measurement point. There is a pressure overshoot at point B, but the overshoot disappears at points C and D. This implies that uniform test flow is achieved from the position marked with C and D, and the test duration is measured to be about 50 μs .

Figure 22 shows pressure histories measured at four measurement points of the second test case where the initial pressure in the FDC driver is set to be 1.5 MPa, being higher than that used in the first case, but all other initial conditions are kept the same. It is observed that the pressure plateau appears at measurement point E. This implies that the uniform test flow is achieved from this position; the test duration is about 70 μs . Actually, it is not sufficient to determine the test time based only on the pressure plateau because there is no pressure change across the contact surface that separates the test gas from the driver gas. In the section on flow visualization, a series of conical shock photographs will be presented to support our test time determination because the temperature will vary across the contact surface.

By comparing Fig. 21 with Fig. 22, we find that the pressure plateau appears later in Case 2. This means that the stronger flow expansion leads to a longer development time of the test flow in the acceleration section. Therefore, high quality test flows can be obtained at different positions for different initial test conditions. According to the observed phenomena, the test section should be movable along the expansion section, so that experiments could be carried out at more uniform test flows of higher quality. Actually, the test flow needs space to

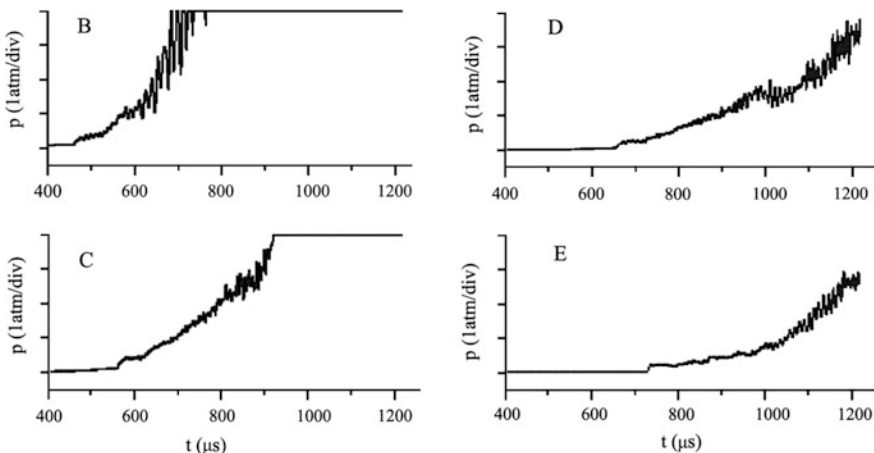


Fig. 22 Wall pressure histories at four measurement points under the initial conditions of 1.5 MPa in FDC driver, 20 mm Hg in the shock tube and 0.15 mm Hg in the acceleration section

develop, the higher the incident shock Mach number is, the longer is the flow expansion distance.

By using the measured incident shock speeds, some key parameters behind the incident shock during the flow development can be calculated with Mirels’ theory. The results at 2 and 4 m positions starting from the second diaphragm along the expansion tube are presented in Table 3. In this table, u_s is the shock speed, u_c is the flow velocity, l_m and l are the maximum and measured distance between the incident shock and the interface behind the shock, respectively. From this table, it can be seen that the flow velocity at 2 m reaches 7190 m/s for Case 1, and 8336 m/s for Case 2. At the 4 m position, the flow velocity is a little lower, but still reached 6971 m/s for Case 1 and 8108 m/s for Case 2. This result implies that the incident shock will decay along the expansion tube due to viscous attenuation.

Table 3 Parameters during the flow development evaluated along the expansion tube at distance of 2 and 4 m from the second diaphragm along the expansion tube

	2 m		4 m	
	Case1	Case2	Case1	Case2
u_s (m/s)	7512	8472	7168	8163
l/l_m	0.51	0.83	0.81	0.99
l_m (mm)	89	25.3	90	25.3
l (mm)	45	21	73	25
u_c/u_s	0.957	0.964	0.973	0.973
u_c (m/s)	7190	8336	6971	8108

4.3 Other Parameters for Expansion Tubes

There are several important parameters in the expansion tube techniques that influence the performance of the JF16 expansion tube. These parameters were investigated, and some results are presented as follows:

The initial pressure in the shock tube was found to be a key parameter and plays an important role in flow stability. Setting the initial pressure in the FDC driver to be 1.0 MPa, several experiments were carried out by setting the shock tube pressure to 10 , 20 and 50 mm Hg. The pressure variations measured at the same position along the shock tube are presented in Fig. 23. It can be seen that the higher the shock tube pressure, the stronger is the flow pressure fluctuations. The pressure ratio across the incident shock wave changes as the shock tube initial pressure varies because of the constant pressure in the FDC driver. This means that the sound speed ratio (the driver gas to the test gas) will change across the incident shock wave, for example, the sound speed ratio is 0.826 in the case shown in Fig. 23a, 0.877 in Fig. 23b, and 1.086 in Fig. 23c, respectively. It is believed that the flow perturbations are generated

Fig. 23 Pressure history profiles measured in the shock tube at different shock tube pressures

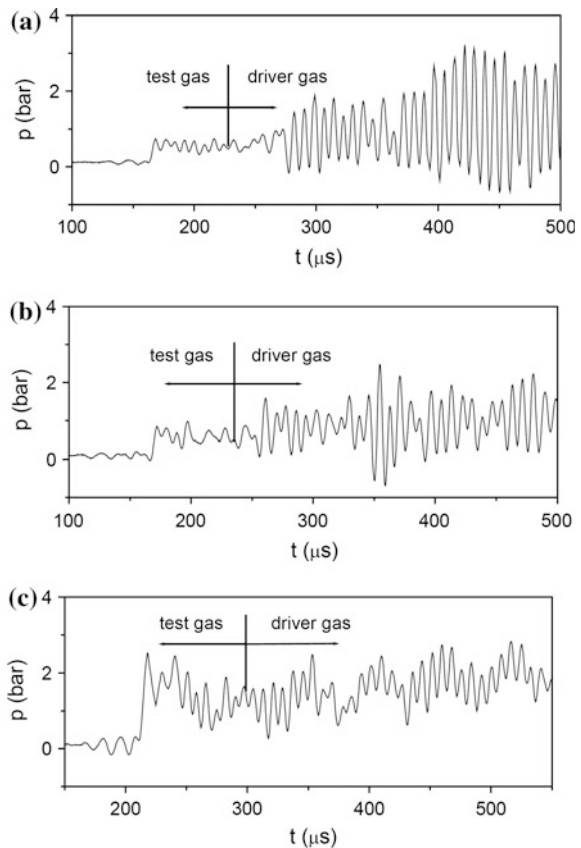
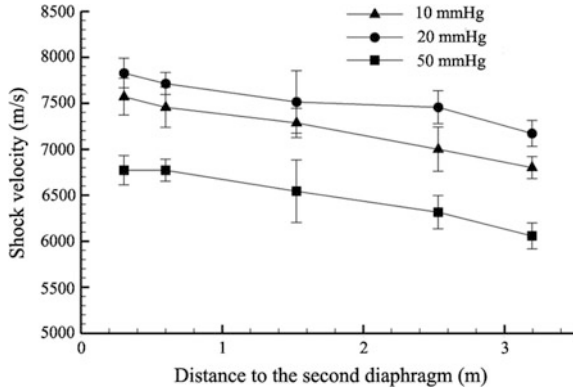


Fig. 24 Incident shock decay along the expansion acceleration tube at different pressures of the shock tube

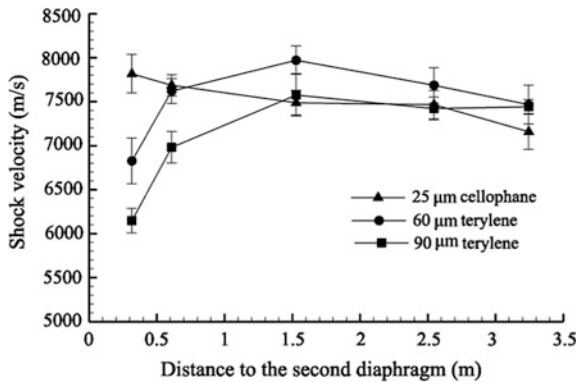


mainly in the driver section and the higher sound speed ratio will lead to stronger perturbations in the driver gas. These perturbations could propagate rapidly into the test gas. Therefore, having the sound speed ratio being less than unity is a good choice for achieving high quality test flows.

The results of the incident shock decay along the expansion acceleration section at different initial shock tube pressures are presented in Fig. 24. It is observed that the decay ratio is almost the same, approximately 3 % per meter, and the incident shock speed reaches its maximum value when the shock tube pressure is taken to be 20 mm Hg. The maximum incident shock speed actually results from the pressure ratio across the primary diaphragm, the flow expansion after the second diaphragm, and their interaction. At present, this mechanism is not clear and more attention should be paid to such a problem when tuning an expansion tube.

The second diaphragm is found to be another important parameter for tuning an expansion tube. By using three kinds of diaphragms with different thicknesses: 90 μm terylene, 60 μm terylene and 25 μm cellophane. The results of the incident shock speed in the expansion tube are presented in Fig. 25. It is observed that the

Fig. 25 Incident shock speed decay along the expansion tube when using different diaphragms



expansion tube performance benefits from the 25 μm cellophane. Thick diaphragms can lead to the shock speed decay upon the diaphragm rupture and flow re-acceleration later, as shown in Fig. 25.

4.4 Test Duration from Flow Visualization

In order to demonstrate the test flow stability and the effective test time, the flow visualization was carried out using a schlieren system and a high-speed camera. Photos of the conical shock in front of a sharp cone are presented in time order in Fig. 26.

In order to obtain the conical shock photographs, a steel 15° sharp cone made of steel is mounted in the test section. The test flow is generated at the condition being the same to Case 2, and the flow velocity is measured to be about 8100 m/s. A FASTCAM SA4 camera is used to for photographing from the test section, while exposure time of 1 μs is used, and the time interval between successive frames is 25 μs . Figure 26a (left hand top figure) shows the photograph taken 25 μs after the incident shock passes. By examining the conical shock angle from Fig. 26b–d, it can be seen that the shock configuration is the same. The flow field in Fig. 26a appears to be light blue, which shows the characteristics of the low-temperature gas filled initially into the expansion acceleration section. The flow field in Fig. 26e appears to be light yellow, which shows the characteristics of the driver gas. This fact indicates that the test flow thus generated is uniform since the shock angle keeps constant from Fig. 26b–d, and the test duration is not shorter than 50 μs , but not longer than 100 μs . Test flow quality is well demonstrated by these flow visualizations. Furthermore, the conical shock configuration is obtained at the flow velocity of 8100 m/s and the total flow enthalpy is about 39 MJ/kg according to the equilibrium theory. Therefore, such photographs are useful for CFD validation since there are no reports of such data at the near orbital speeds.

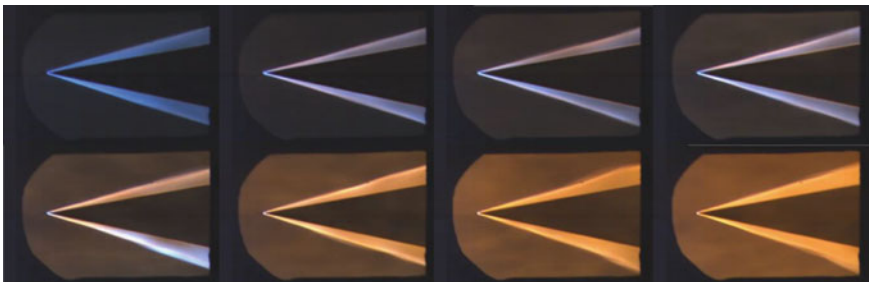


Fig. 26 Sequential photos of conical shocks in front of a 15° sharp cone placed in 8100 m/s hypersonic flow (the time interval is 25 μs between successive frames and the exposure time is 1 μs)

4.5 *Concluding Remarks*

The detonation-driven high-enthalpy expansion tube was developed successfully by combining up-to-date techniques of the detonation driver with an expansion acceleration section. The hypervelocity test flow of over 8 km/s and a total enthalpy up to 40 MJ/kg is generated in this facility for conducting experiments at the near orbital speed. From its performance tests, the hypervelocity flow was demonstrated to be relatively uniform and this indicates that the high quality test flow could be achieved by using the FDC driver. Experimental results also demonstrated that the ratio of the sound speeds across the driving and test gas interface has a critical impact on the magnitude of test flow perturbations, but the perturbations can be suppressed to a certain extent if the ratio does not exceed unity. The maximum velocity of the test flow can be obtained by adjusting the filling pressure of the shock tube while maintaining constant filling pressures in both the detonation driver and the expansion acceleration section. This implies that the optimization of test conditions is possible for the performance of the JF16 expansion tube in addition to the facility configuration optimization. Experiments also showed that the second diaphragm affects both the gas dynamics and the chemical kinetics of the test gas and the JF16 expansion tube performance benefits from light and thin diaphragms.

5 *Summary*

The first enclosed wind tunnel was invented in 1871 to measure the drag over a solid body by Wenham, a Council Member of the Aeronautical Society of Great Britain. Many wind tunnels for various purposes have been built in the world since then. Nowadays, to develop innovative flying vehicles, the wind tunnels become larger and larger in size, and require more and more high level of power for tunnel operation. For hypersonic flow generation, the power needed is so huge that the blow-down wind tunnels could not be employed to replicate the correct velocity or enthalpy that is necessary for hypersonic experiments. Because of the power limitation on continuous wind tunnels, shock tunnels were developed for ground-based hypersonic experiments. As the development of numerous advanced measurement techniques continues, the application of hypersonic shock tunnels is expected to become wider and wider. Detonation-driven high-enthalpy and hypersonic test facilities have been developed in the State Key Laboratory of High Temperature Gas Dynamics (LHD), Institute of Mechanics, Chinese Academy of Sciences (CAS), for years. The typical trajectories of various spacecrafts can be covered with these facilities and research on aero-thermo-dynamics and hypersonic propulsion can be carried out to gain a fundamental understanding on hypersonic physics. More especial is the long-test-duration hypervelocity detonation-driven shock tunnel (JF12) that is capable of duplicating the flight condition for Mach number 5–9 at an altitude of 25–50 km. The hypervelocity flow region of more than two

meters in diameter can be generated for test duration more than 100 ms at reasonable operation cost.

The detonation is the violent combustion and its rapid energy conversion in explosives is the property which is very useful. A 20 m² detonation front operates at a power level equal to the total power the earth receives from the sun. The FDC driver and the backward-running detonation driver combining with a dump section make use of the detonation successfully and provide shock tunnels with the required power level at affordable expense. Techniques proposed for extending shock tunnel test duration are of significant importance because the long test duration cannot be achieved only by increasing shock tunnel length. Detonation-driven high-enthalpy and hypersonic test facilities so far developed and based on the present shock tunnel techniques demonstrated its several good properties, such as the stable reservoir pressure, the required enthalpy level, the long test duration and the cheap operation cost. These properties are very good for generating hypervelocity flows for ground tests. However, the heat transfer from detonated gases to facilities and the facility damage due to the harsh thermo-environment occur in the detonation-driven facilities, being even more severe. For advanced hypersonic test facilities, the detonation-driven shock tunnels are very promising, but their improvement both in its design and operation is necessary in future.

Acknowledgments The author would like to acknowledge the National Natural Science Foundation of China which provides funding for this research under the projects of 10632090 and 10621202. The authors would like to thank all the members from the group of shock wave and detonation physics for their kind assistance in experiments and facility development.

References

1. Bertin, J.J.: Hypersonic Aerothermodynamics. AIAA Education Series, Washington DC (1994)
2. Park, C.: Nonequilibrium Hypersonic Aerothermodynamics. Wiley, New York (1990)
3. Anderson, J.D.: Hypersonic and High Temperature Gas Dynamics. McGraw-Hill Book Company, New York (1989)
4. Bertin, J.J., Cummings, R.M.: Fifty years of hypersonics: Where we've been, where we're going. *Prog. Aerosp. Sci.* **39**, 511–536 (2003)
5. Hirschel, E.H.: Viscous effects. In: *Space Course 1991*, vol. 12, pp. 1–35, Aachen
6. Bertin, J.J., Cummings, R.M.: Critical hypersonic aerothermodynamic phenomena. *Ann. Rev. Fluid Mech.* **38**, 129–157 (2006)
7. Lu, F.K., Marren, D.E.: *Advanced Hypersonic Test Facility (198)*. Progress in Astronautics and Aeronautics, Reston (2002)
8. Holden, M.S.: Design, development and calibration of the LENS facility (pp. 94–0161). AFOSR-TR (1994)
9. Holden, M.S., Wadhams, T.P., Candler, G.V.: A review of experimental studies in the LENS shock tunnel and expansion tunnel to examine real-gas effects in hypervelocity flows. In: 42th AIAA Aerospace Sciences Meeting and Exhibit Reno, AIAA Paper 2004-0916, NV, 5-8 Jan 2004

10. Holden, M.S., Chadwick, K.M., Kolly, J.M.: Hypersonic studies in the LENS facilities, AIAA 95-6040. In: 6th International Aerospace Planes and Hypersonic Technologies Conferences, Chattanooga, Tennessee, 3–7 April 1995
11. Stalker, R.J.: A study of the free-piston shock tunnel. *AIAA J.* **5**, 2160–2165 (1967)
12. Stalker, R.J., Morrison, W.R.B.: New generation of free piston shock tunnel facilities. In: Proceeding of the 17th International Symposium on Shock Tube and Waves, Bethlehem (1989)
13. Hornung, H.G.: The piston motion in a free-piston driver for shock tubes and tunnels, GALCIT Rep. FM88-1, 1988
14. Itoh, K., Ueda, S., Komuro, T., et al.: Improvement of a free piston driver for a high-enthalpy shock tunnel. *Shock Waves* **8**, 215–233 (1998)
15. Itoh, K., Ueda, S., Tanno, H., Komuro, T., Sato, K.: Hypersonic aerothermodynamic and scramjet research using high enthalpy shock tunnel. *Shock Waves* **12**, 93–98 (2002)
16. Bird, G.A.: A note on combustion driven tubes. Royal Aircraft Establishment, vol. 146, AGARD Report, May 1957
17. Yu, H.: Recent developments in detonation drivers. In: Proceedings of the Fifth National Symposium on Shock Waves and Shock tubes, Xi'an, China, Nov 1988
18. Yu, H., Esser, B., Lenartz, M., Grönig, H.: Gaseous detonation driver for a shock tunnel. *Shock Waves* **2**, 245–254 (1992)
19. Olivier, H., Jiang, Z., Yu, H., Lu, F.K.: Detonation driven shock tubes and tunnels Advanced Hypersonic Test Facilities, pp. 135–203. AIAA, USA (2002)
20. Jiang, Z., Yu, H., Takayama, K.: Investigation into converging gaseous detonation drivers. In: Ball, G.J., Hillier, R., Roberts, G.T. (eds.) Proceedings of ISSW22, Shock Waves, London, UK, 18–23 July 1999
21. Jiang, Z., Zhao, W., Wang, C., Takayama, K.: Forward-running detonation drivers for high-enthalpy shock tunnels. *AIAA J.* **40**, 2009–2016 (2002)
22. Zhao, W., Jiang, Z., Saito, T., Lin, J.M., Yu, H.R., Takayama, K.: Performance of a detonation driven shock tunnel. *Shock waves* **14**(1–2), 53–59 (2005)
23. Jiang, Z., Lin, J., Zhao, W.: Performance tests of JF-10 high-enthalpy shock tunnel with a FDC driver. *J. Hypersonics* **2**(1), 29–35 (2011)
24. Jiang, Z., Yu, H.: Experiments and development of long-test-duration hypervelocity detonation-driven shock tunnel (LHDst). AIAA paper 2014-1012 (2014)
25. Jiang, Z., Gao, Y., Zhao, W.: Performance study on detonation-driven expansion tube. AIAA paper 2009-7237 (2009)
26. Li, J.P., Feng, H., Jiang, Z., Yu, H.R.: Numerical computation on the tailored shock Mach numbers for a hydrogen/oxygen detonation shock tube. *Acta Aerodynamica Sinica* **26**, 291–296 (2008)
27. Li, J.P., Feng, H., Jiang, Z.: Investigation into test gas contamination of shock tunnels induced by shock/boundary interactions. *Acta Mechanica Sinica* **40**, 289–296 (2008)
28. Jiang, Z., Li, J.P., Zhao, W., Liu, Y.F., Yu, H.R.: Investigation into techniques for extending the test-duration of detonation-driven shock tunnel. *Chinese Journal of Theoretical and Applied Mechanics* **44**, 824–831 (2012)
29. Laderman, A.L.: Shock-tube performance with area divergence at the diaphragm section. *AIAA Journal* **10**, 1904–1906 (1967)
30. Resler, E.L., Bloxson, D.E.: Very High Mach Number Flows by Unsteady Flows Principles. Cornell University, Graduate School of Aeronautical Engineering, New York (1952)
31. Trimpi, R.L.: A preliminary theoretical study of the expansion tube: A new device for producing high-enthalpy short duration hypersonic gas flows. NASA TR-133 (1962)
32. Neely, A.J., Stalker, R.J., Paull, A.: High enthalpy hypervelocity flows of air and argon in an expansion tube. *Aeronaut. J.* **95**(946), 175–186 (1991)
33. Sasoh, A., Morgan, R.G., et al.: High-enthalpy expansion tube experiments with gas injection. *AIAA J.* **38**, 2253–2259 (2000)

Author Biographies



Zonglin Jiang is well known for his studies in shock wave and detonation physics, cutting-edge technologies for the long-test-time shock tunnel and hypervelocity shock-expansion tube, and numerical algorithms for shock-capturing. He has authored/coauthored hundreds of journal papers by far. He received his PhD degree from Peking University in 1993, and has been the director of State Key Laboratory of High-temperature Gas Dynamics since 2000. He and his team set up a large scale shock tunnel with a test time up to 130 milliseconds in 2011. He is now Professor of Institute of Mechanics, Chinese Academy of Sciences, President of International Shock Wave Institute, and Vice President of Chinese Aerodynamics Research Society. His current research interests include detonation initiation and propagation, hypersonic gas dynamics and propulsion, as well as hypersonic and hypervelocity test technology.



Hongru Yu is a famous scientist in aerodynamics who has been concentrating on studies of the theory, experiment and application of shock tube/tunnel. After graduating from Dalian Institute of Technology in 1953, he joined the university as a lecturer. He moved to Institute of Mechanics, Chinese Academy of Sciences (IMCAS) in 1957. Prof. Yu initiated the study on shock tube/tunnel technology at IMCAS and developed the first shock tube and the first shock tunnel in China with his research group in 1960s. He also expedited detonation-driver technology for the development of high-enthalpy shock tunnels during 1980s. Since 1991, he has been an academican of Chinese Academy of Sciences.